An Acad Bras Cienc (2023) 95(Suppl. 2): e20220762 DOI 10.1590/0001-3765202320220762
Anais da Academia Brasileira de Ciências | *Annals of the Brazilian Academy of Sciences*
Printed ISSN 0001-3765 I Online ISSN 1678-2690
www.scielo.br/aabc | www.fb.com/aabcjournal

ENGINEERING SCIENCES

Comparative study on ignition delay time and burning rate of modified double-base propellant and fuel-rich propellant

LIAN-BO LI, TAO CHEN, WEI-XUAN LI & RONG-FU YU

Abstract: With the higher requirements of various tactical and technical indicators of the weapon systems, the current research on the ignition and combustion characteristics of different types of solid propellants is not comprehensive. In more complex and harsh environmental conditions, the pressure affects the ignition and combustion characteristics. Therefore, the paper studies the ignition and combustion characteristics of the modified double-base propellants (MDB propellants) and fuel-rich propellants (FR propellants) under low-pressure environment. Combining experiment and theory, the ignition delay time and burning rate of two kinds of solid propellants are compared and analyzed at low pressure by the laser ignition experimental device. The results displayed that the burning flames of the FR and MDB propellant presented evident V-shape and cylindrical, respectively. The flame brightness decreased with the decrease in pressure. With the increase of pressure and heat flux, the ignition delay time of the MDB propellant and the FR propellant decreased. By comparison, Model 2 of the ignition delay time was more effective for the estimation of the ignition delay time of the FR propellant. The experimental results are compared with the three burning rate models, which are the Vielle formula (Model 1), Summerfield formula (Model 2), and B-number burning rate formula (Model 3). The results showed the burning rate was more in accord with Model 3.

Key words: Burning rate, ignition delay time, fuel-rich propellant, modified double-base propellant, laser ignition.

INTRODUCTION

With technological advancements of missile weapons and space delivery equipment, the power propulsion performance has become an essential indicator for measuring the performance of modern weapons and space delivery systems. As the power source of propulsion systems, the solid propellant's ignition process and combustion performance have an important influence on the working characteristics and interior ballistic characteristics. The study of the solid propellant's ignition process and combustion performance is helpful in revealing its combustion mechanism, provides reference data for the establishment and verification of propellant ignition models, and has important guiding significance for the performance prediction of the propulsion system.

As early as the 1960s, many scholars began to research the ignition and combustion process of solid propellants, including ignition theory, experimental methods, combustion theory, combustion process, the factors which affect ignition and combustion performance, and put forward the theoretical

models of ignition and combustion of a variety of propellants. Although they were not perfect, they still had specific application values (Chaturvedi & Dave 2019, Arkhipov et al. 2015). The laser ignition method had the advantages of high output energy, controllable ignition time, concentrated energy, and difficult attenuation during the transmission process, which was suitable for the ignition and combustion research of solid propellants under low-pressure environment. Kakami et al. (2008), Kakami & Tachibana (2015) conducted laser radiation ignition on the double-base propellant, analyzed the law of temperature change on the burning surface, and found that the laser energy density in the ignition process accords with the Gaussian distribution. Herreros & Fang (2017) used a diode laser to study the laser ignition of the elastomer modified cast double-base propellants. The experimental results showed that the smaller the laser beam width and the larger the laser pulse width, the shorter the ignition delay time. The higher the laser power, the shorter the burning time of the propellants, and there is an ignition threshold during the ignition process. Xiao et al. (2020) studied the effect of aluminum on the combustion performance of the modified double-base propellant, and observed the flame structure, combustion surface phenomenon and the morphology of the extinguishing surface. Zarzecki et al. (2013) studied the ignition delay time and the combustion process of PMMA under different ambient pressures and oxygen concentrations, and measured the burning rate of PMMA by the target line method. The experimental results showed that the burning rate decreased continuously with the decrease of pressures, and increased with the increase of oxygen concentrations. Hedman et al. (2013), Hedman (2016) used CO_2 lasers to carry out laser ignition experiments on solid propellants with different compositions, and compared the pyrolysis rate, flame structure and burning time. The experimental results showed that the flame height and flame brightness decreased with the increase of ambient pressures.

With the advancement of propulsion technology, many scholars proposed adding metals to solid propellants to increase their energy. Fuel-rich propellants were then gradually developed. Ao et al. (2020) conducted ignition and combustion experiments to study the agglomeration, ignition and combustion characteristics of aluminum-based alloy solid composite propellant, which provided a theoretical basis for selecting alloy elements to improve the combustion performance of aluminum-based alloy solid composite propellant. Pang et al. (2020) researched the reaction mechanism of ferric hydroborate compounds in AP / HTPB / Al composite solid propellant and its effect on the combustion performance. The experimental results showed that the flame of the HTPB solid propellant containing ferric hydroborate compound presented a multi-flame structure under different pressures, and the flame temperature changed with the pressure. Liu et al. (2020) conducted in-depth experimental research on the influence of RDX content on combustion and agglomeration performances using laser ignition, thermogravimetry differential scanning calorimetry and combustion diagnosis methods. The experimental results showed that the addition of RDX inhibited the decomposition of AP, improved the ignition delay time and the self-sustaining burning time of the aluminized propellants, and reduced the burning rate. Vo et al. (2018) established a motion boundary model that contained a solid zone and a gas zone of the solid propellant system. Lee et al. (2019) and Meredith et al. (2015) established a detailed numerical model for the laser-induced ignition reaction of HMX to simulate the ignition, combustion and flameout process of HMX / gap solid propellants in a rocket motor. Zhang et al. (2017) conducted experimental observations on the HTPB propellant containing AP particles using laser ignition, and recorded the combustion process,

and measured the burning rate with a high-speed camera. A new burning rate model based on the heat balance equation was established. The solid and gas conservation equations were solved. The experimental results of Sivan & Haas (2015) indicated that the difference in ignition delay time not only depended on the fuel and oxidant, but to a greater extent depended on the chemical reaction occurring in the gas phase and solid phase, but had nothing to do with the decomposition temperature of the oxidizer.

Few studies conducted to compare the performance of modified double-base propellants and fuel-rich propellants. Therefore, the motivation of this paper is to investigate the effect of pressure on the ignition and combustion performance of these two propellants. Firstly, the laser ignition experimental system, the experimental conditions and the composition of the two propellants are introduced. Secondly, the influences of pressure on flame structure, ignition delay time and burning rate are mainly studied. Finally, the effect law of pressure on the ignition delay time and burning rate of the two propellants is summarized, and the comparative analysis of the ignition delay time models and burning rate models is carried out respectively.

EXPERIMENTAL SYSTEM

The laser ignition experimental system is mainly composed of CO2 laser, chamber, vacuum pump, data acquisition module and controller. Its schematic diagram is shown in Fig. 1. The laser wavelength is $10.6\ \mu m$. The diameter of the laser beam spot is $\varnothing 3.5\ mm$. The combustion chamber size is $150 \times 150 \times 300\ mm$, with glass windows in the front and back. The limit pressure of the vacuum pump (RVP-6) is 4×10^{-2} Pa. The shooting speed of the high-speed camera which is Sanyo HD2000 is 240 frames per second.

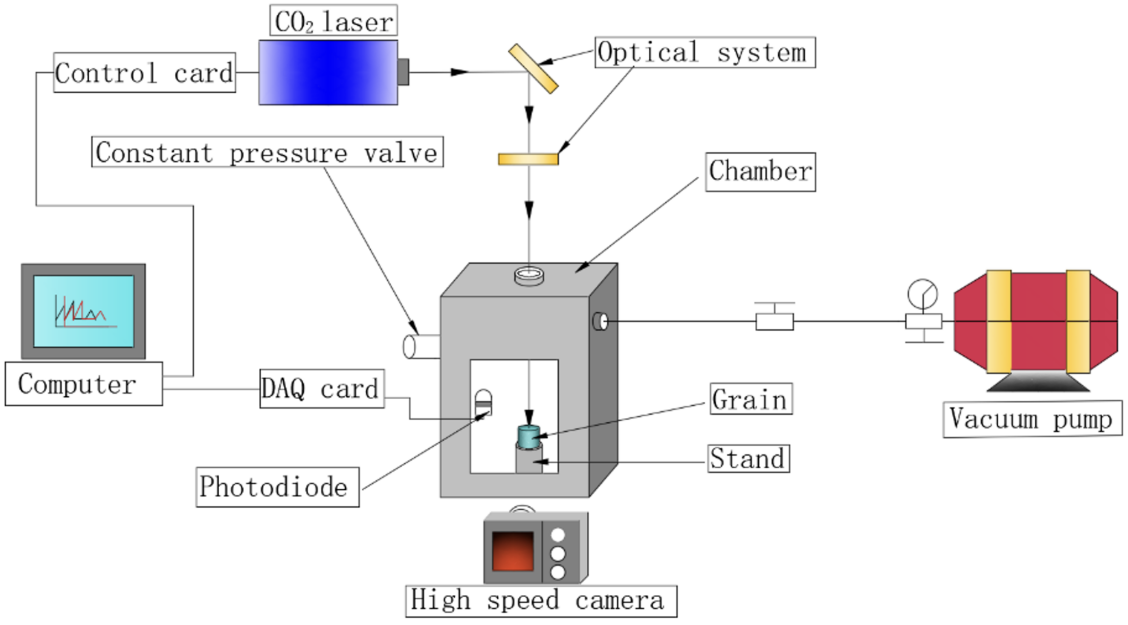

Figure 1. The schematic diagram of the laser ignition experimental system.

In the laser ignition experiment system, the vacuum pump is connected to the combustion chamber which is kept airtight after the test sample is placed. Using the vacuum pump to extract the air gas, the pressure in the combustion chamber is lower than the standard atmospheric pressure. The controller adjusts the laser loading time and laser power. After passing through the light path adjustment module, the laser irradiates the test sample in the combustion chamber vertically. Using two photodiodes to monitor the flame signal and laser signal, the ignition delay time can be obtained. One photodiode is positioned in the chamber wall to monitor the flame signal. The second photodiode is positioned at the laser generator to monitor the laser signal. The two optical signals are converted into a voltage signal and recorded by the acquisition card. The response time of the photodiodes is extremely short, and the ignition delay time error caused by the photodiodes is negligible. The gas produced by the combustion of the propellants can change the pressure in the combustion chamber. In order to keep the pressure in the combustion chamber constant, the acquisition card monitors the pressure in real-time using the pressure sensor, and transmits it to the computer to compare with the working pressure which is set before the experiment. The computer calculates the feedback data to the controller, which controls the closing of the solenoid valve and the pumping rate of the vacuum pump to keep the pressure in the combustion chamber constant. A high-speed camera is used to photograph the ignition and combustion process of the propellants. The total burning time was obtained to calculate the linear burning rate of the propellants. In order to reduce the experimental error and ensure the accuracy of experimental data, the tests were carried out five repeated under each working condition.

SPECIMEN

FR propellants have the characteristics of low oxidant content and high metal agent content. Due to the high oxygen poor degree, the performance and combustion process of FR propellants have their own characteristics. The basic components of FR propellants include oxidant (ammonium perchlorate, abbreviation of AP), polymer binder (hydroxyl-terminated polybutadiene, abbreviation of HTPB), metal additives (aluminum and magnesium powder, Al and Mg) and a small amount of other additives, such as curing agent, antioxidant, combustion stabilizer and plasticizer. The modified double-base propellant is widely used in tactical weapons because of its high energy, excellent manufacturing process, good storage performance and good performance. The main formula of the modified double-base propellant includes HMX-50%, NC-20%, NG-20%, 3,4-dinitrofurazanyl furoxan(DNTF)-6%, N-methyl-4-nitroaniline (MNA)-1%, elastic stabilizer-1.5% and catalyst-1.5%. The compositions of the fuel-rich propellant and the modified double-base propellant used in this paper are shown in Table I. In the experiment, two kinds of solid propellants are sheared into a cylinder with a diameter of $\varphi 5\ mm$ and $5\ mm$ in length. In order to obtain accurate experimental data and clear experimental phenomena, the cylindrical surface of the specimen is coated with high temperature resistant insulating rubber to prevent the specimen from burning sideways.

Five repeated tests under the same experimental conditions led to a change in ignition time of $\pm 30\ ms$. Under the test conditions, the external heat flux is $0.3\ W/mm^2$, $1.2\ W/mm^2$, $2.8\ W/mm^2$, and the pressure from 0.02 MPa to 0.08 MPa. Table II lists the experimental conditions of this paper.

Table I. Composition of FR propellant and MDB propellant.

Type	Component	Mass fraction	Type	Component	Mass fraction
FR propellant	AP	36.0%	MDB propellant	HMX	50.0%
	HTPB	20.0%		NC	20.0%
	Al	20.0%		NG	20.0%
	Mg	20.0%		DNTF	6.0%
	Others	4.0%		MNA	1.0%
				Others	3.0%

Table II. List of test conditions.

Test conditions	Values
Pressure (MPa)	0.02, 0.04, 0.06, 0.08
Oxygen concentration (%)	21
External heat flux $\left(W/mm^2\right)$	0.3, 1.2, 2.8
Inlet air temperature $(^{\circ}C)$	20

FLAME STRUCTURE

The ignition and combustion processes of the FR propellants and MDB propellants are very similar. The entire combustion process was recorded by the high-speed camera which is Sanyo HD2000 at a frame rate of 240 frames per second. Compared with the volume of the combustion chamber, the sample is too small. When the sample is totally gasified, the pressure and oxygen content of the combustion chamber change little. Therefore, the change of oxygen concentration in the combustion chamber is not considered in the experiment. The typical flame images of the FR propellant and MDB propellant under different pressures are shown in Figs. 2-3. The results show that the flame shape and brightness differ in low-pressure environments.

In Fig. 2, when the pressure is 0.08 MPa, the flame of the FR propellant is stronger and brighter. However, the flame is darker and the upper part of the flame oscillates violently and disorderly under the pressure of 0.04 MPa and 0.02 MPa. When the pressure is higher, the combustion is more sufficient and the flame becomes brighter and stronger. When the pressure is lower, the flame darkens, which is easy to cause the flame swing disorder. In the early stage of the combustion process, a cylindrical initial flame is formed above the propellant burning surface at 0.08 MPa, a spot-like initial flame is formed at 0.04 MPa, a spherical initial flame is formed at 0.02 MPa. In the later stage of the combustion process, it can be clearly seen that the flame separates and forms a multi-stranded shape, in a V-shape. This is because the flame model of Al-Mg FR propellant belongs to the divergent model (Yan et al. 2009). This phenomenon is more obvious when the pressure is 0.02 MPa, because the aluminum particles in the propellant are instantaneously heated and agglomerated to form aluminum droplets, which flow with the gas and form a flame jet (Liu et al. 2020).

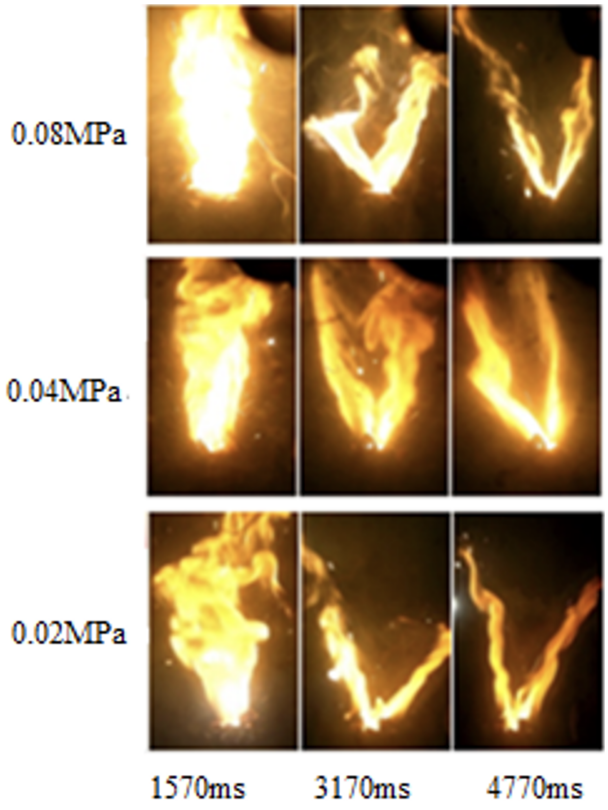

Figure 2. Flame structure of FR propellant under different pressures.

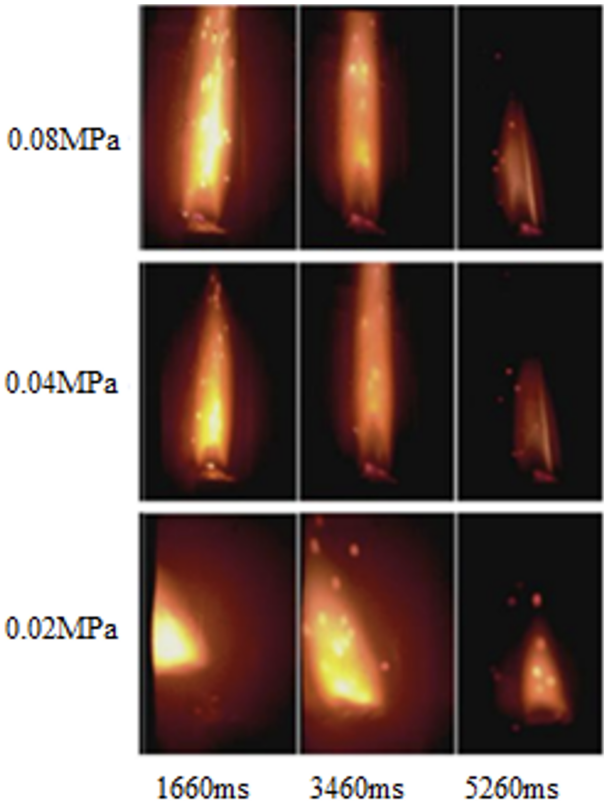

Figure 3. Flame structure of MDB propellant under different pressures.

In Fig. 3, the flame shape of the MDB propellant is cylindrical under the pressure of 0.08 MPa, and there are incomplete burnt sparks in the flame. When the pressure is 0.04 MPa, the flame brightness decreases obviously, and the flame shape is unstable. When the pressure is 0.02 MPa, the flame is very unstable, and the propellant can self-sustaining combustion, but the flame is easy to extinguish by repeated jumping. It can also be seen that when the pressure is 0.08 MPa, the density of the pyrolysis products produced by the thermal decomposition of the MDB propellant is lower than that of air, forming a columnar diffusion zone, and the propellant is ignited rapidly. When the pressure is reduced to 0.04 MPa, the axial diffusion decreases due to the lower pressure and thinner air. The pyrolysis gas diffuses irregularly in the area above the propellant surface. The ignition delay time increases. As the pressure decreases further, the irregular diffusion effect becomes more obvious. Therefore, the difference of flame shape and brightness is due to the influence of ambient pressure on the diffusion of pyrolysis gas. When the pressure is high, the pyrolysis gas mainly diffuses along the axial direction due to the effect of buoyancy. With the decrease of pressure, the pyrolysis gas begins to diffuse irregularly around. As the pressure continues to decrease, the irregular diffusion becomes more obvious, which is consistent with the results of the literature (Naya & Kohga 2014).

IGNITION DELAY TIME

Ignition delay time is an important parameter to measure the quality of the ignition process (Burke et al. 2015). In the laser ignition experiment system, the data acquisition system uses two photodiodes to collect the laser signal and initial flame signal, respectively. The collected signals are transmitted to the computer through the data acquisition card. One photodiode collects the laser signal and converts it into electrical signals. After, the initial flame signal is detected by the other photodiode, and converted into electrical signals. The ignition delay time is defined as the time interval from which the laser signal to the photodiode surveys the initial flame signal. The typical electrical signal curve of the laser ignition process is shown in Fig. 4. The laser loading time is 1270ms, which is less than the burning time of the propellant specimen.

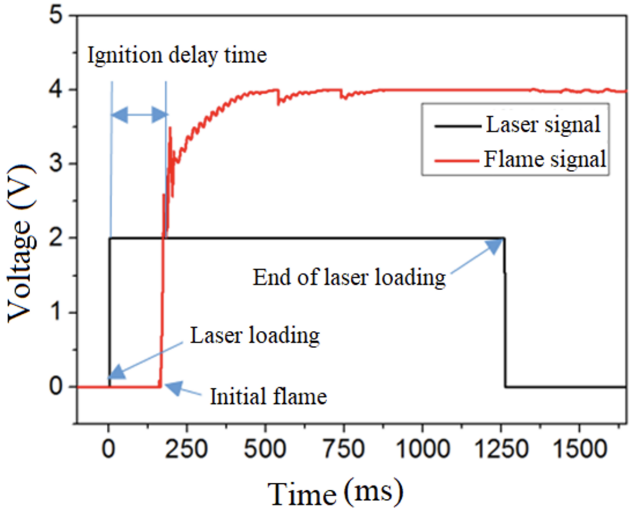

Figure 4. Electrical signal curve during the ignition process.

In this study, the authors analyze in detail the factors that affect the ignition delay time. According to the authors' previous research results, ignition delay time t_{ig} is composed of a pyrolysis time (t_{py}), a mixing time (t_{mix}) and a gas phase chemical reaction time (t_{chem}).

$$t_{ig} = t_{py} + t_{mix} + t_{chem} \tag{1}$$

The pyrolysis reaction occurs when the propellant is heated to a sufficiently high temperature. When the pyrolysis gas is sufficient to allow piloted ignition, the conduction heating time is t_{py}. Based on the thermal theory, t_{py} is inversely proportional to the quadratic power of the laser heat flux density (Li et al. 2018), $t_{py} \propto \frac{1}{q_0^2}$. q_0 is laser heat flux density. It shows that the greater the heat flux density of the laser irradiated on the propellant surface, the shorter the pyrolysis time. When enough energy is obtained, the chemical reaction of the combustible mixture will enter a "thermal runaway" or a flaming condition. The piloted ignition time is called t_{chem}. According to the heat transfer and chemical kinetics laws t_{chem} is inversely proportional to the quadratic power of the pressure (Li et al. 2018), scilicet, $t_{chem} \propto \frac{1}{p^2}$. During the mixing process of pyrolysis gas and ambient gas, the diffusion or

transport time required for the fuel and oxygen concentration to ignite is called t_{mix}. It can be inferred that the mixing time t_{mix} is a function of the 1/2 power of the pressure.

In order to better analyze the influence of ambient pressure on the ignition delay time of different kinds of solid propellants, the experimental data can be fitted according to the above theoretical analysis model. In the above theoretical analysis of ignition delay time, according to the laws of heat transfer and chemical kinetics, t_{chem} is inversely proportional to the square of pressure. Combined with the mathematical model of pressure and ignition delay time established by Zarzecki et al. (2013), the above mathematical model is modified to make it more consistent with the ignition characteristics of the solid propellants. In this experiment, the laser heat flux, oxygen concentration (21%) and initial temperature (20°C) are fixed values, and the relationship between ignition delay time and pressure can be expressed as:

$$t_{ig} = a_1/p^2 + b_1 \tag{2}$$

which is called Model 1 in this paper. In Formula (2), p is the pressure of combustion chamber, MPa; a_1 is the ignition delay time coefficient of Model 1, $ms \cdot MPa^2$; b_1 is called as the adjustment coefficient of Model 1, ms.

According to the theoretical analysis, the mixing time t_{mix} is a function of the 1/2 power of the pressure. In this experiment, the laser heat flux, oxygen concentration (21%) and initial temperature (20°C) are fixed values, so the relationship between ignition delay time and pressure can also be expressed as:

$$t_{ig} = b_2 - a_2 p^{0.5} \tag{3}$$

which is called Model 2 in this paper. In Formula (3), a_2 is the ignition delay time coefficient of Model 2, $ms \cdot MPa^{0.5}$; b_2 is called as the adjustment coefficient of Model 2, ms.

According to Formula (2) and Formula (3), the mean test results (five tests for each working condition) are fitted using Ordinary Least Squares, respectively. The fitting curves under different laser heat fluxes are shown in Fig. 5, and the fitting results are listed in Table III. The experimental data of the ignition delay time of the FR propellant and the MDB propellant under different low pressure are shown in Fig. 5. The results show that the ignition delay time decreases with the increase of pressure and heat flux. However, compared with the MDB propellant, the heat flux has more significant influence on the ignition delay time of the FR propellant than the pressure. If the pressure is reduced, the diffusion rate of the pyrolysis products into the surrounding environment will be increased, and the collision frequency and chemical reaction rate between molecules will be reduced, so that the chemical reaction area is far away from the propellant surface. At the same time, when the exothermic reaction zone moves away from the propellant surface, the thermal feedback on the propellant surface will be reduced, resulting in a longer ignition delay time (Hou et al. 2021, Zhang et al. 2020).

Table III shows the fitting results of theoretical models Model 1 and Model 2 with experimental data. It can be seen that for the fuel-rich propellant, the relationship between ignition delay time and ambient pressure is more consistent with the Model 2, indicating that the Model 2 is more effective for the calculation of the ignition delay time of the FR propellant in low-pressure environment. As far as the MDB propellant, the fitting results of theoretical models Model 1 and Model 2 are similar. When the heat flux is high, the fitting effect of Model 1 is better. When the heat flux is low, the fitting effect of Model 2 is better. When the laser heat flux is low, the inert heating time is longer. Therefore, the FR

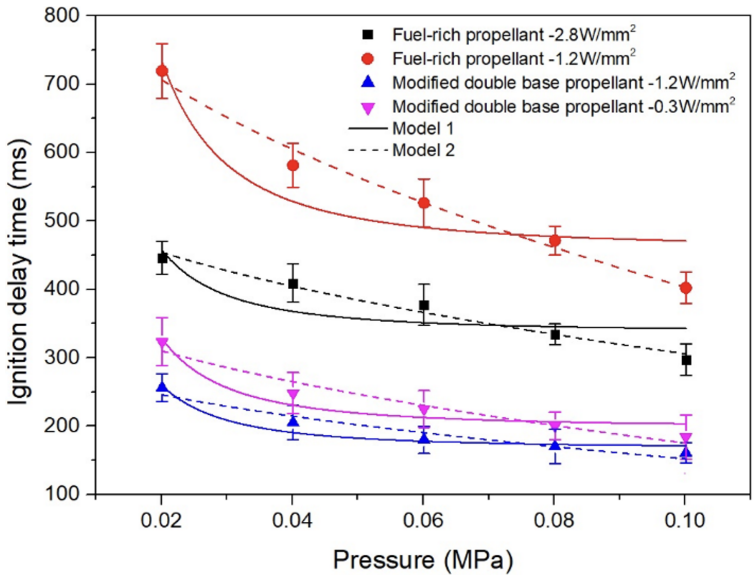

Figure 5. The variation of ignition delay time with pressure under different heat fluxes.

Table III. Fitting results of ignition delay time under different pressure.

Model	Formula	Propellant type	Heat flux (W/mm^2)	Fitting parameters	Correlation coefficients R^2
Model 1	$t_{ig} = a_1/p^2 + b_1$	Fuel-rich propellants	2.8	a_1 = 0.04758; b_1 = 339.77779	0.54926
			1.2	a_1 = 0.10931; b_1 = 461.80584	0.79125
		Modified double base propellants	1.2	a_1 = 0.03668; b_1 = 169.55383	0.92176
			0.3	a_1 = 0.05181; b_1 = 200.08166	0.89917
Model 2	$t_{ig} = b_2 - a_2 p^{0.5}$	Fuel-rich propellants	2.8	a_2 = 849.06734; b_2 = 575.90381	0.97334
			1.2	a_2 = 1732.995; b_2 = 952.6726	0.981
		Modified double base propellants	1.2	a_2 = 536.21185; b_2 = 323.52948	0.91353
			0.3	a_2 = 771.50578; b_2 = 420.91489	0.93725

propellant and the MDB propellant show a tendency that with the decrease of heat flux, the influence of the pressure on the ignition delay time becomes larger and larger.

In summary, by comparing the ignition delay time of the FR propellant and the MDB propellant under low pressure, it can be seen that the FR propellant has poorer ignition performance, and requires higher ignition energy. When the laser heat flux is $1.2\ W/mm^2$, the ignition delay time of the FR propellant is as high as about 500 ms. However, the MDB propellant requires lower ignition energy, which can also be ignited when the laser heat flux is as low as $0.3\ W/mm^2$, and the maximum ignition delay time is about 300 ms. Therefore, the MDB propellant has better ignition performance. At the same time, it can be seen that the pressure has different effects on the ignition delay time of the FR propellant and the MDB propellant. When the ambient pressure increases from 0.02 MPa to 0.1 MPa, the variation range of ignition delay time of the FR propellant is about 750 ms-500 ms, while the variation range of ignition delay time of the MDB propellant is about 250 ms-150 ms. Therefore, when the combustion chamber pressure changes, the ignition delay oscillation of the FR propellant is larger, while the ignition delay time of the MDB propellant changes less and is more stable. Therefore, the MDB propellant has better ignition characteristics, such as low ignition energy, less influence by pressure and stable ignition.

BURNING RATE

As we all know, the commonly used formulas to characterize the burning rate of the solid propellants include the Vielle burning rate formula and the Summerfield burning rate formula, as follows:

Vielle burning rate formula:

$$\dot{r} = a_v \cdot p^n \tag{4}$$

Summerfield burning rate formula:

$$\frac{1}{\dot{r}} = \frac{a_s}{p} + \frac{b_s}{p^{\frac{1}{3}}} \tag{5}$$

where, $\dot{r}$ is the burning rate, $mm \cdot s^{-1}$; p is the pressure in the combustion chamber, MPa; a_v is the burning rate coefficient of the Vielle formula, $mm \cdot s^{-1} \cdot \mathrm{MPa}^{-n}$; n is the burning rate pressure index; a_s and b_s are the burning rate coefficients of Summerfield formula, a_s represents the influence of various factors other than pressure on the chemical reaction rate, $s \cdot \mathrm{MPa}/mm$, and b_s represents the influence of various factors other than the pressure on the diffusion mixing effect, $s \cdot \mathrm{MPa}^{1/3}/mm$.

Based on the B number theory (Quintiere 2006), the burning rate formula is further deduced in this paper. When the solid propellants burn stably without an external heat source, the energy balance equation on the propellant surface is expressed as

$$q = q_{f,c} + q_{f,r} - \sigma\left(T_v^4 - T_\infty^4\right) \tag{6}$$

where, $q_{f,c}$ is flame convective heat flux, $q_{f,r}$ is flame radiative heat flux, $\sigma\left(T_v^4 - T_\infty^4\right)$ is surface radiative heat loss, σ is Stefan–Boltzmann constant, T_v is gasification temperature of the propellant surface, T_∞ is ambient temperature. q is the net heat flux of propellant surface, and is equal to the energy flux of the fuel vaporization, which can be estimated by the heat of gasification L.

$$q = \dot{r}\rho_s L \tag{7}$$

Reference (Li et al. 2018) found that the flame convective heat flux and flame radiative heat flux are both affected by the ambient pressure. Specifically, the flame convective heat flux can be expressed as a function of the **1/2** power of the ambient pressure, and the flame radiative heat flux can be expressed as the quadratic function of the ambient pressure, which is

$$q_{f,c} = function\left(p^{1/2}\right) \tag{8}$$

$$q_{f,r} = function\left(p^{2}\right) \tag{9}$$

Through simplified analysis, the radiative heat loss of the thin-layer flame can be expressed as

$$\sigma\left(T_v^4 - T_\infty^4\right) = \dot{r}\rho_s \Delta h_c X_r \tag{10}$$

where, ρ_s is solid density, X_r is radiative fraction of the flame, Δh_c is heat of combustion. As can be seen from the above derivation, $q_{f,c}$ is proportional to $p^{1/2}$, and $q_{f,r}$ is proportional to p^2. Thus, $q_{f,c} + q_{f,r}$ is a function of $p^{1/2}$. Eq. (8), (9), (10) are substituted into Eq. (7), which is converted to Eq. (11). The experimental data are fitted by Eq. (11), which shows that the burning rate and square root of pressure is a power function. Therefore, B-number burning rate formula is expressed as

$$\dot{r} = function\left(p^{1/2}\right) = a_B + b_B\left(p^{1/2}\right)^c \tag{11}$$

where, a_B is the burning rate adjustment coefficient of the B-number burning rate formula, $mm \cdot s^{-1}$; b_B is the burning rate coefficients of the B-number burning rate formula, $mm \cdot s^{-1} \cdot \mathrm{MPa}^{-c/2}$; c is the burning rate pressure index of the B-number burning rate formula.

In the laser ignition experiment system, the burning rate of the FR propellant and the MDB propellant was measured under different low-pressure environments. Under the pressure of 0.02 MPa, 0.04 MPa, 0.06 MPa, 0.08 MPa and 0.1 MPa respectively, the burning rate of the FR propellant and the MDB propellant varies with the pressure, as shown in Fig. 6. Each node in the figure represents the average value of 5 times measurement results under the same experimental conditions. It can be clearly seen from the experimental measurement that the burning rate of the FR propellant and the MDB propellant increases with the increase of the pressure. The increase of pressure can cause the burning rate to increase significantly with the heat flux, because the surface convective heat flux and radiant heat flux increase as the pressure increases. As the pressure decreases, the burning rate decreases. When the ambient pressure decreases from 0.1 MPa to 0.02 MPa, the burning rate decreases by 47%. This may be caused by the different energy and efficiency of thermal feedback: (1) in the lower pressure environment, the oxygen concentration is lower, the burning intensity is weakened, resulting in the lower flame temperature, so that the thermal feedback energy from flame zone to solid zone is reduced; (2) in the lower pressure environment, the gas thermal conductivity decreases, which reduces the thermal feedback efficiency from the flame zone to the solid zone. Since the solid-phase thermal decomposition of the propellant is an endothermic reaction, the reduction of the thermal feedback energy and efficiency reduces the solid-phase thermal decomposition rate, which leads to a decrease in the burning rate.

Vielle equation (Model 1), Summerfield equation (Model 2) and B-number burning rate equation (Model 3) are respectively used to fit and analyze the burning rate data under different low-pressure environments. The fitting curve is shown in Fig. 6, and the relevant fitting parameters are shown in

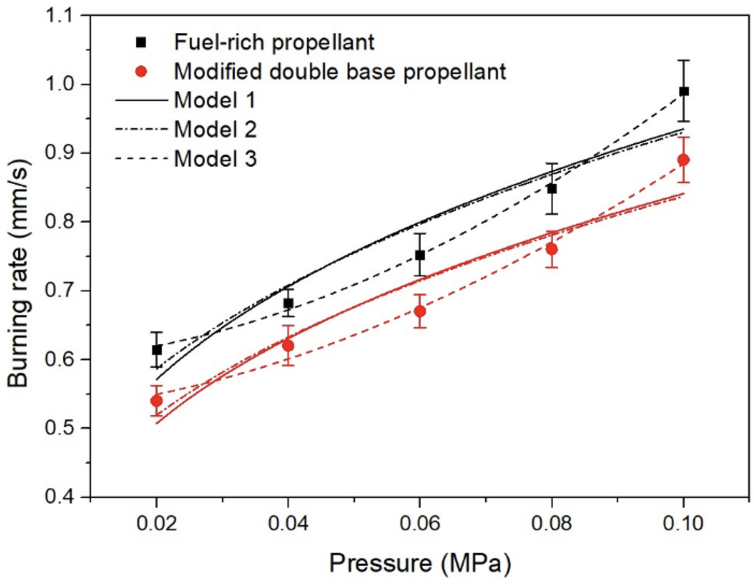

Figure 6. **Burning rate fitting curve under different pressure environment.**

Table IV. **Fitting results of burning rate under different pressure.**

Model	Formula	Propellant type	Fitting parameters	Correlation coefficients R^2
Model 1	$\dot{r} = a_v \cdot p^n$	Fuel-rich propellants	a_v = 1.89199; n = 0.30628	0.87149
		Modified double base propellants	a_v = 1.73397; n = 0.31436	0.88397
Model 2	$\frac{1}{\dot{r}} = \frac{a_s}{p} + \frac{b_s}{p^{\frac{1}{3}}}$	Fuel-rich propellants	a_s = -0.00402; b_s = 0.51813	0.88547
		Modified double base propellants	a_s = -0.0035; b_s = 0.57142	0.89296
Model 3	$a_B + b_B\left(p^{1/2}\right)^c$	Fuel-rich propellants	a_B = 0.59902; b_B = 25.57062; c = 3.64037	0.99479
		Modified double base propellants	a_B = 0.52717; b_B = 18.86254; c = 3.44577	0.98278

Table IV. According to the fitting curve and fitting coefficient, it can be seen that compared with Vielle equation (Model 1) and Summerfield equation (Model 2), the B-number burning rate equation (Model 3) fits better with the experimental data. It shows that although the burning rate model established in this paper simplifies the comprehensive influence of ambient pressure on the burning rate, the theoretical model is effective for the burning rate of the FR propellant and the MDB propellant. Therefore, in low-pressure environment, the B-number burning rate equation is more suitable for characterizing the burning rate characteristics of the FR propellant and the MDB propellant. At the same time, it can also be seen that compared with the MDB propellant, the B-number burning rate equation has a better fitting effect on the burning rate of the FR propellant.

CONCLUSION

In order to improve the reliability and applicability of propulsion system at high altitude, the ignition and combustion characteristics of two commonly used solid propellants (FR propellants and MDB propellants) at low pressure were studied. The flame structure, ignition delay time and burning rate under different low pressure and laser heat flux were studied by the laser ignition experiment system. The experimental results of the influence of pressure on ignition delay time and burning rate showed that the pressure affects the diffusion of the propellant pyrolysis gas, resulting in the difference in the shape and brightness of the burning flame. The lower the pressure, the lower the flame height and the worse the brightness. The flame of the FR propellant is stronger and brighter than that of the MDB propellant. The flame shape of the MDB propellant is cylindrical. In the later stage of the combustion process, it can be clearly seen that the flame of the FR propellant separates and forms a multi-stranded shape, in a V-shape. The ignition delay time increases with the decrease of pressure, but the influence of pressure on ignition delay time decreases significantly with the increase of heat flux. Comparing the experimental measurements with Model 1 and Model 2 of the ignition delay time, the results showed Model 2 is more accurate in estimating the ignition delay time. Compared with the FR propellant, the MDB propellant has better ignition characteristics, requires lower ignition energy, is less affected by pressure, and has stable ignition. The pressure has a great influence on the burning rate. As pressure increase, the burning rate increased. Through the comparison of Vielle formula (Model 1), Summerfield formula (Model 2) and B-number burning rate formula (Model 3), it can be seen that B-number burning rate formula (Model 3) is more suitable for characterizing the FR propellant and the MDB propellant. Model 3 shows that the functional relationship between pressure and burning rate, and the fitting result is consistent with the experimental measurements. This is because the increase in pressure facilitates the heat transfer, radiation and convection of the flame, which makes the propellant sample ignite and burn faster.

Acknowledgments

This research was supported by Scientific Research Foundation of Nanjing Vocational University of Industry Technology (No. YK20-01-11), China Postdoctoral Science Foundation (Certificate Number: 2023M731674) and Jiangsu Funding Program for Excellent Postdoctoral Talent.

REFERENCES

AO W, FAN Z, LIU L, AN Y, REN J, ZHAO M, LIU P & LI LK. 2020. Agglomeration and combustion characteristics of solid composite propellants containing aluminum-based alloys. Combust Flame 220: 288-297.

ARKHIPOV V, SAVEL'EVA L & ZOLOTOREV N. 2015. Effect of aluminum-boron powders mechanical mixtures on the combustion of high-energy materials at subatmospheric pressures. In: MATEC Web of Conferences. France: EDP Sciences, Vol. 23, p. 01005.

BURKE U, SOMERS KP, O'TOOLE P, ZINNER CM, MARQUET N, BOURQUE G, PETERSEN EL, METCALFE WK, SERINYEL Z & CURRAN HJ. 2015. An ignition delay and kinetic modeling study of methane, dimethyl ether, and their mixtures at high pressures. Combust Flame 162(2): 315-330.

CHATURVEDI S & DAVE PN. 2019. Solid propellants: AP/HTPB composite propellants. Arab J Chem 12(8): 2061-2068.

HEDMAN TD. 2016. Radiation-induced pyrolysis of solid fuels for ramjet application. Propuls Power Res 5(2): 87-96.

HEDMAN TD, GROVEN LJ, LUCHT RP & SON SF. 2013. The effect of polymeric binder on composite propellant flame structure investigated with 5 kHz OH PLIF. Combust Flame 160(8): 1531-1540.

HERREROS DN & FANG X. 2017. Laser ignition of elastomer-modified cast double-base (EMCDB) propellant using a diode laser. Opt Laser Technol 89: 21-26.

HOU Y, XU J, ZHOU C & CHEN X. 2021. Microstructural simulations of debonding, nucleation, and crack propagation in an HMX-MDB propellant. Mater Des 207: 109854.

KAKAMI A, HIYAMIZU R, SHUZENJI K & TACHIBANA T. 2008. Laser-Assisted combustion of solid propellants at low pressures. J Propul Power 24(6): 1355-1360.

KAKAMI A & TACHIBANA T. 2015. Heat balance evaluation of double-base solid propellant combustion using thermography and laser heating on a burning surface. Aerosp Sci Technol 47: 86-91.

LEE GH, JUNG MY, YOO JC, MIN BS, SHIM HM & OH M. 2019. Dynamic simulation of ignition, combustion, and extinguishment processes of HMX/GAP solid propellant in rocket motor using moving boundary approach. Combust Flame 201: 129-139.

LI LB, CHEN X, MUSA O, ZHOU CS & ZHU M. 2018. The effect of pressure and oxygen concentration on the ignition and combustion of aluminum-magnesium fuel-rich propellant. Aerosp Sci Technol 76: 394-401.

LIU H, AO W, HU Q, LIU P, HU S, LIU L & WANG Y. 2020. Effect of RDX content on the agglomeration, combustion and condensed combustion products of an aluminized HTPB propellant. Acta Astronaut 170: 198-205.

MEREDITH KV, GROSS ML & BECKSTEAD MW. 2015. Laser-induced ignition modeling of HMX. Combust Flame 162(2): 506-515.

NAYA T & KOHGA M. 2014. Influences of particle size and content of RDX on burning characteristics of RDX-based propellant. Aerosp Sci Technol 32(1): 26-34.

PANG WQ, DELUCA LT, FAN XZ, GLOTOV OG, WANG K, QIN Z & ZHAO FQ. 2020. Combustion behavior of AP/HTPB/Al composite propellant containing hydroborate iron compound. Combust Flame 220: 157-167.

QUINTIERE JG. 2006. Fundamentals of fire phenomena .

SIVAN J & HAAS Y. 2015. Laser ignition of various pyrotechnic mixtures–an experimental study. Propellants Explos Pyrotech 40(5): 755-758.

VO ND, JUNG MY, OH DH, PARK JS, MOON I & OH M. 2018. Moving boundary modeling for solid propellant combustion. Combust Flame 189: 12-23.

XIAO LQ, FAN XZ, LI JZ, QIN Z, FU XL, PANG WQ & WANG Y. 2020. Effect of Al content and particle size on the combustion of HMX-CMDB propellant. Combust Flame 214: 80-89.

YAN QL, LI XJ, WANG Y, ZHANG WH & ZHAO FQ. 2009. Combustion mechanism of double-base propellant containing nitrogen heterocyclic nitroamines (I): the effect of heat and mass transfer to the burning characteristics. Combust Flame 156(3): 633-641.

ZARZECKI M, QUINTIERE JG, LYON RE, ROSSMANN T & DIEZ FJ. 2013. The effect of pressure and oxygen concentration on the combustion of PMMA. Combust Flame 160(8): 1519-1530.

ZHANG H, LIU M, MIAO Y, WANG H, CHEN T, FAN X & CHANG H. 2020. Dynamic mechanical response and damage mechanism of HTPB propellant under impact loading. Materials 13(13): 3031.

ZHANG L, TIAN R & ZHANG Z. 2017. Burning rate of AP/HTPB base-bleed composite propellant under free ambient pressure. Aerosp Sci Technol 62: 31-35.

How to cite
LI L-B, CHEN T, LI W-X & YU R-F. 2023. Comparative study on ignition delay time and burning rate of modified double-base propellant and fuel-rich propellant. An Acad Bras Cienc 95: e20220762. DOI 10.1590/0001-3765202320220762.

Manuscript received on September 10, 2022;
accepted for publication on March 5, 2023

LIAN-BO LI[1]
https://orcid.org/0000-0003-4026-7634

TAO CHEN[2]
https://orcid.org/0009-0009-1627-0017

WEI-XUAN LI[3]
https://orcid.org/0000-0002-1936-4918

RONG-FU YU[4]
https://orcid.org/0009-0005-7783-354X

[1]Nanjing Vocational University of Industry Technology, School of Mechanical Engineering, Yangshan North Road Street, 1, 210023 Nanjing, China
[2]Nanjing Institute of Technology, School of Energy and Power Engineering, Chunhua Street, n/n, 211167 Nanjing, China
[3]Nanjing University of Science and Technology, School of Mechanical Engineering, Xiaolingwei Street, n/n, 210094 Nanjing, China
[4]Jiangsu Focusun Refrigeration CO., LTD, Hailing Street, n/n, 225300 Taizhou, China

Correspondence to: **Tao Chen**
E-mail: 2020101116@niit.edu.cn

Author contributions

Lian-bo Li and Wei-xuan Li conducted experiments and established mathematical models for ignition delay time and combustion rate. Tao Chen and Rong-fu Yu conducted experimental data processing.